SUPPLEMENTARY MATERIAL

Resolution of Established Cardiac Hypertrophy and Fibrosis and Prevention of Systolic Dysfunction in a Transgenic Rabbit Model of Human Cardiomyopathy Through Thiol-sensitive Mechanisms

Raffaella Lombardi, MD. PhD., Gabriela Rodriguez, MD., Suet Nee Chen, MS., Crystal M. Ripplinger, PhD.#, Wenwen Li, PhD.#, Junjie Chen, PhD.#, James T Willerson, MD., Sandro Betocchi, MD.*, Samuel A. Wickline, MD.#, Igor R. Efimov, PhD.#, AJ Marian, MD.

Center for Cardiovascular Genetic Research, Brown Foundation Institute of Molecular Medicine, The University of Texas Health Science Center, and the Texas Heart Institute, Houston, TX 77030

* Department of Clinical Medicine, Cardiovascular and Immunological Sciences, Federico II University of Naples, Naples, Italy.

Department of Biomedical Engineering, Washington University in St. Louis, MO

AJ Marian, MD
Center for Cardiovascular Genetic Research
The Brown Foundation Institute of Molecular Medicine
The University of Texas Health Science Center
6770 Bertner Street, DAC 900A
Texas Heart Institute at St. Luke's Episcopal Hospital
Houston, TX 77030
Direct: 713 500 2350
Indirect: 713 500 2345, 713 500 2312
713 500 2320 (Fax)
Ali.J.Marian@uth.tmc.edu

MATERIAL AND METHODS

The investigation conforms to the *Guide for the Care and Use of Laboratory Animals* published by the US National Institutes of Health (NIH Publication No. 85-23, revised 1996) and was approved by the Institutional Animal Care and Use Committee.

β-MyHC-Q403 transgenic rabbits: We have published generation and phenotypic characteristics of the β-MyHC-Q403 transgenic rabbits [1;2]. In brief, phenotypic expression of HCM is age-dependent [2]. It is fully expressed in 2- year rabbits, age of enrollment in this study [2]. At the age of 2 years, the transgenic rabbits exhibit cardiac hypertrophy, interstitial fibrosis, myocyte disarray and preserved global systolic function. Older rabbits (3-4 years old) gradually exhibit a modest decline in global systolic function, as detected by the measurement of left ventricular fractional shortening and Doppler indices [2].

Placebo-controlled study and administration of N-acetylcysteine (NAC): The study groups included age- sex- and body weight-matched adult non-transgenic rabbits (N=10), β-MyHC-Q403 transgenic rabbits assigned to a placebo (drinking water, N=10) and β-MyHC-Q403 transgenic rabbits treated with NAC at the dosage of 500mg/Kg (N=10). We selected the dosage of NAC according to our previous data in a mouse model of HCM showing reversal of cardiac fibrosis after treatment with NAC [3] as well as other data [4;5]. The duration of the treatment was 12 months, selected because of the slowly evolving nature of cardiac hypertrophy in HCM.

Measurement of blood and myocardial levels of oxidized and total glutathione: We measured levels of oxidized glutathione (GSSG) and of total glutathione [reduced glutathione (GSH) plus GSSG) in the whole blood by a spectrophotometric method using a commercially available kit (Calbiochem, EMD Chemicals Inc., affiliate of Merck KGaA, Darmstadt, Germany, cat#371757) per manufacturer's instructions (N=6 rabbits per group). In brief, we first converted all glutathione molecules in the sample to GSH by adding the enzyme glutathione reductase and nicotinamide adenine dinucleotide phosphate (NADPH). Then, we added 5,5'-dithiobis-2-nitrobenzoic acid (DTNB) to the reaction, which

in the presence of GSH forms 5-thio-2-nitrobenzoic acid (TNB), a product that is quantifiable by spectrophotometry. We then determined TNB levels by measuring the absorbance at 412 nM. We recorded the change in adsorbance for 3 minutes and calculated the rate of TNB production, which is directly proportional to the concentration of GSH in the sample.

To quantify GSSG levels, we removed the GSH in the sample by adding 1-methyl-2-vinylpyridinium trifluoromethane-sulfonate (M2VP). M2VP rapidly scavenges GSH by forming a stable complex. Then, we reduced GSSG to GSH and measured the GSH levels as described above.

Likewise, we measured myocardial levels of oxidized and total glutathione in 50 mg aliquots of freshly isolated ventricular tissues using the above kit. We homogenized the tissues in 250 μl of lysis buffer and added 10% M2PV to the lysis buffer to scavenge the GSH when measuring GSSG. We collected the supernatant and added equal volume of deproteination reagent (5% Metaphosphoric Acid; MPA). We used 50 μL of the mixture in the assay.

M mode, two dimensional and Doppler echocardiography: We performed echocardiography using a H-P Sonos 5500 unit equipped with a 8MHz transducer as published [2;6-8]. An investigator without knowledge of group assignment analyzed the images.

Morphometric analysis of myocyte cross sectional area (CSA), collagen volume fraction (CVF) and myocyte disarray: We performed the morphometric analyses of myocyte CSA, percent of CVF and percent of myocardium showing myocyte disarray by semi-automated planimetry in age- and sex- and body weight-matched non-transgenic, transgenic rabbits in the placebo group and transgenic rabbits in the NAC group, as described [2;6;7]. In brief, to quantify myocyte CSA, we placed freshly harvested thick cardiac cross-sections in optimal cutting temperature (OCT) compound (Sakura-Finetek U.S.A. Inc., Torrace, CA) and froze them in liquid nitrogen. We prepared thin myocardial sections, washed in PBS for 3 times and stained with Wheat Germ Agglutinin (WGA)

conjugated with Texas Red (*W21405*; Molecular Probes Inc., Eugene, OR, cat # W21405) at the working concentration of 2 μg/mL for 1 hour at room temperature. After the incubation, we washed the sections 3 times in PBS and mounted the section in Fluorescence Mounting Medium (Biomeda Corp., Foster City, CA). We divided each thin section into 48 approximately equal fields and sampled 48 high magnification (x400) microscopic fields per each thin section and 5 thin sections per heart to measure myocyte CSA (approximately 12,000 myocytes) in 4 rabbits per group. To test for reproducibility of the measurement of the myocyte CSA, we randomly selected 20 thin myocardial sections and repeated the measurements without knowledge of the group assignment in two different occasions.

To quantify CVF, we stained formalin-fixed 5-μm-thick sections with collagen-specific Sirius red F3BA. We quantified percent of positive stained areas in approximately 240 high magnification fields per each heart (N=6 per group). We excluded perivascular and epimysial collagens from the analysis. We also determined intra-observer variability of the measurement of CVF by repeating the measurements in 20 randomly selected thin myocardial sections on two different occasions.

We quantified percent of myocyte disarray as described previously [2;6;7]. We divided thin H & E stained myocardial sections into 48 fields of approximately equal size, and scored the presence or absence of disarray in each field. We computed the number of fields showing disarray in each section as a percent of the total number of fields in a total of 480 fields per heart (N=6 per group). We excluded areas of the myocardium at the junctions of interventricular septum with the ventricles, sections near the blood vessels, trabeculations and the papillary muscles from the analysis. To test the reproducibility of quantification of myocyte disarray, we quantified the percent of myocyte disarray in 40 randomly selected thin myocardial sections without knowledge of the group assignment in 2 different occasions.

Diffusion-Weighted Magnetic Resonance Imaging (DTMRI): We performed DTMRI on 3.7% formaldehyde-perfused hearts as published recently [9;10]. In brief, we

calculated myofiber helix angle (α) for a mid left ventricular short axis slice at 10 steps across the left ventricular wall from epi- to endocardium in four 20°-wide sectors at the anterior, lateral, inferior, and septal regions. We then calculated the fiber angle for the entire slice as the average of these four regions (N=4 per group).

Thiol-sensitive signaling kinases and phosphatases: We determined levels of active (dephosphorylated) form of Nuclear Factor of Activated T cells (NFATc) in nuclear proteins extracts from the hearts using a commercially available ELISA Kit (cat #40296, Active Motif, Carlsbad, CA). The well in the 96-well plate were coated with an oligonucleotide containing NFATc consensus binding site (5-AGGAAA-3´). Aliquots of 10 μg of total nuclear protein extracts were loaded into each sample-well. After incubation for 1 hour at room temperature with mild agitation, to allow for the DNA binding, we washed the wells and added a mouse monoclonal primary antibody against an accessible epitope on NFATc1 protein at a 1:500 dilution and incubate for 1 hour at room temperature. After three washes, we added a secondary anti mouse IgG HRP-conjugated antibody at 1:1000 dilution and incubate for 1 hour at room temperature. After 8 minutes of incubation in TMB developing solution, we stopped the reaction by adding H2SO4 and measured the adsorbance within 5 minute at 450 nm.

We determined activities of cyclic guanosine 3',5'-monophosphate (cGMP)-dependent protein kinase (PKG) a commercially available ELISA kit (CycLex., Ltd, Ina-Nagano, Japan, distributed by MBL International Woburn, MA, cat # CY-1161). The assay contains 96-well plates whose wells are coated with the specific protein kinase substrate. We loaded equal amounts of total proteins (50 μg) into each sample-well and incubated the reaction in the respective activation buffers. After washing the wells, we then added a phospho-specific antibody recognizing the phosphorylated substrate (mouse monoclonal HRP-conjugated anti-phospho-G-kinase substrate, 10H11 antibody) for 1 hour at room temperature. The primary antibody was already conjugated with HRP; therefore, after three washes, the

assay was incubated in developing solution (tetra-methylbenzidine (TMB)). The reaction was stopped after 15 minutes by adding 0.5 N sulphuric acid (H2SO4) and the adsorbance was read at dual wavelengths of 450/540 nm.

We detected and quantified expression levels of total and phosphorylated extracellular signal regulated kinases (ERK) 1-2, p38 and Jun N-terminal kinases (JNK) 54/46 by immunoblotting using pan-specific and phospho-specific antibodies (Santa Cruz Biotechnology Inc., Santa Cruz, CA and for phosphor-JNK54/46 Cell Signaling Technology Inc., Danvers, MA) in 4-6 rabbits per group. We froze the heart tissues by placing them in liquid nitrogen and homogenized them in the RIPA Lysis Buffer [1X formulation, 25 mM Tris-HCl pH 7.6, 150 mM NaCl, 1% NP-40, 1% Sodium deoxycholate and 0.1 % sodium dodecyl sulphate (SDS, cat# 89900, Pierce Biotechnology, Rockford, IL)]; and complete protease and phosphatase inhibitor cocktails, (cat # 11-697-498-001 and 04-906-845-001, respectively, Roche Diagnostics, GmbH, Mannheim, Germany]. We determined the protein concentration using Coomassie Protein Reagent (Pierce Biotechnology, Rockford, IL) by the Bradford protein assay. We loaded aliquots of 30 μg of protein extracts onto SDS-polyacrylamide gels, separated the proteins by electrophoresis and transferred them to nitrocellulose membranes.

We probed the membranes with antibodies against: total ERK (goat polyclonal IgG sc-94-G, at 1:500 dilution); p-ERK (mouse monoclonal IgG2a, sc-7383, at 1:200 dilution); total p38 (goat polyclonal IgG, sc-535-G at 1:100 dilution); p-p38 (mouse monoclonal IgM, sc-7973, at 1:100 dilution); total JNK (goat polyclonal IgG, cat#9255, at 1:200 dilution); p-JNK (mouse monoclonal IgG1, Cell Signaling cat# 9255, at 1:100 dilution). The secondary antibodies were: goat anti mouse IgG-horseradish peroxidase (HRP) conjugated (sc-2005, at 1:3000 dilution for p-ERK, 1:1000 dilution for p-JNK); goat anti mouse IgM-HRP (sc-2064 at 1:2000 dilution); donkey anti goat IgG-HRP (sc-2033, at 1:3000 dilution for total ERK, 1:1000 dilution for total p38 and total JNK). Finally, the membranes were stripped in Restore PLUS Western blot stripping buffer (Pierce, Rockford, IL, cat#21059) and probed

with a mouse monoclonal antibody IgG2a fragment against α-tubulin (sc-5286 at 1:1000 dilution) as the primary antibody and a goat anti-mouse HRP-conjugated IgG antibody, as the secondary antibody (sc-2005, 1:2000 dilution). The signals were detected by chemiluminescence (ECL detection reagents and Hyperfilm by Amersham Bioscience, Piscataway, NJ, cat # RPN-2106 and 28-9068-37, respectively) and analyzed to measure the intensity of the detected bands by spot densitometry.

Glutathiolation of cardiac α-actin: We detected and quantified glutathiolation of cardiac α-actin by co-immunoprecipitation, under non-reducing conditions. In brief, we added 4 µg of anti-human cardiac α-Actin monoclonal antibody (CAA, clone: Ac1-20.4.2, IgG1 isotype, RDI – Fitzgerald Industries International Inc., Concord, MA), to each 500 µg aliquot of total protein extracts and incubated the reaction on a rocker platform at 4°C overnight. Then, we added 20 µl of Protein A/G PLUS-Agarose beads (sc 2003; Santa Cruz Biotechnology, Santa Cruz, CA) to the solution and incubated the reaction on a rocker platform at 4°C overnight. After centrifugation at 1,000 g for 5 min at 4°C, we washed the precipitate three times by resuspension in ice-cold PBS plus complete protease inhibitors cocktail (Roche Diagnostics, GmbH, Mannheim, Germany, cat # 11-697-498-001) and re-centrifugation. We suspended the final pellet in 50 µl of loading buffer, consisting of Laemmli Buffer (63mM Tris-HCl, pH:6.8, 25% glycerol, 2% SDS, 0.01% brome phenol blue). The samples in loading buffer were heated at 95-100°C for 5 min, subjected to electrophoresis on 10% SDS polyacrylamide gels and transferred to nitrocellulose membranes. We detected the glutathiolated cardiac α-actin by using a mouse monoclonal anti-GSH antibody (1:1000 dilution, , Virogen, Watertown, MA, cat # 101-A-100) and an anti-mouse IgG HRP conjugated secondary antibody (Santa Cruz Biotechnology Inc., Santa Cruz, CA; sc-2005) followed by chemiluminescence reaction (N=4 or 5 per group).

Nuclear G-actin: To detect and localize G-actin, we stained thin myocardial sections with DNase 1, which is known to preferentially bind to monomeric (G) actin as opposed to F-actin (N=4 per group) [11]. In brief, thin frozen heart sections were stained with a

fluorescent conjugate of bovine pancreatic DNase I at 15 μg/ml concentration for one hour at room temperature (Alexa Fluor 594, Molecular Probes Inc., Eugene, OR, cat #D12372). The sections were then washed and mounted in Fluorescence Mounting Medium containing 4',6-diamidino-2-phenylindole (DAPI) (Vector Laboratories, Burlingame, CA, cat #H1500).

Subcellular fractionation of cardiac α-actin: To determine whether glutathiolation of cardiac α-actin affected subcellular localization of actin, we extracted nuclear and cytosolic proteins per a published protocol [12]. In brief, we performed all steps for protein extraction at 4°C, unless specified. We homogenized 200 mg aliquots of minced heart tissues in pre-chilled dounce glass tubes in ice-cold 250-STMDPS buffer [250 mM sucrose, 50 mM Tris-HCl (pH 7.4), 5 mM $MgCl_2$, 1 mM DTT plus proteinase inhibitors cocktail, (cat # 11-697-498-001, Roche Diagnostics, GmbH, Mannheim, Germany)]. We centrifuged the homogenates at 800g for 15 min to collect the supernatant (cytosolic I) and repeated the steps to collect the supernatant again (cytosolic II). We centrifuged cytosolic I and II fractions at 6,000 g for 15 min to pellet the mitochondria. We then combined the two supernatants, centrifuged it at 22,000 g for 1 hour and collected the new supernatant as cytosolic proteins fraction.

To collect nuclear proteins, we resuspended the pellets from the above steps in 300 μl of 2M-STMDPS buffer [2 M sucrose, 50 mM Tris-HCl (pH 7.4), 5 mM $MgCl_2$, 1 mM DTT plus proteinase inhibitors cocktail], homogenized and filtered it through a 100-micron pores nylon mesh to remove debris. After layering the suspension onto a cushion of 2 M STMDPS buffer and centrifugation in a swing-bucket ultracentrifuge at 80,000g for 35 min, we separated the pure nuclei pellets in 2 volumes of a buffer containing 20mM HEPES (pH 7.9), 1.5 mM $MgCl_2$, 0.5M NaCl, 0.2mM EDTA and 20% glycerol plus proteinase inhibitors cocktail. Following incubation for 30 min with gentle rocking, we lyzed the nuclei by passing (x10) through an 18-gauge needle and collected the nuclear protein fraction by centrifugation at 9,000g for 30 min.

We extracted membrane and cytoskeletal proteins using a commercially available kit (Chemicon Int., Danvers, MA; cat #2145). In brief, we homogenized aliquots of 100 mg of minced heart tissues in dounce glass homogenizers in 5 volumes of a cold buffer containing HEPES (pH7.9), MgCl2, KCl, EDTA, Sucrose, Glycerol, Sodium OrthoVanadate plus protease inhibitors cocktail. After incubation for 20 min with gentle rocking, we centrifuged the homogenates at 18,000g for 20 min to pellet membranes, nuclei and cytoskeletal fractions. We separated the nuclei from membrane and cytoskeletal proteins by resuspending the pellets in 100 μl of an ice cold buffer containing HEPES (pH7.9), $MgCl_2$, NaCl, EDTA, Glycerol, Sodium OrthoVanadate, plus proteinase inhibitors cocktail, gentle mixing for 20 min and centrifugation at 18,000g for 20 min. We then resuspended the pellet in 100 μl of a cold buffer containing HEPES (pH7.9), $MgCl^2$, KCl, EDTA, Sucrose, Glycerol, Sodium deoxycholate, NP-40, Sodium OrthoVanadate plus protease inhibitors cocktail and following incubation for 20 min with gentle rocking we centrifuged the homogenate at 18,000 g for 20 min to collect the supernatant containing membrane proteins fraction.

To collect the cytoskeletal protein fraction, we resuspended pellet in 50 μl of a buffer containing Pipes (pH6.8), MgCl2, NaCl, EDTA, Sucrose, SDS, Sodium OrthoVanadate plus protease inhibitors cocktail. We incubated the reaction for 20 min with gentle rocking at room temperature followed by centrifugation at 18,000 g for 20 min. We collected the supernatant containing the cytoskeletal protein fraction and repeated the step to collect the remaining cytoskeletal proteins.

Protein degradation: We analyzed protein degradation in the experimental groups by assessing Calpains 1/2 and the 20S Proteasome activities using two fluorometric commercially available kits (Calbiochem, EMD Chemicals Inc., affiliate of Merck KGaA, Darmstadt, Germany cat# QIA 120, and Chemicon Temecula, CA, cat #APT 280, respectively,). Both assays are based on the detection of the fluorophore 7-Amino-4-methylcoumarin (AMC) which is released upon cleavage from the substrate Suc-LLVY-AMC,

in the presence of calpain or 20S Proteasome containing samples. The assays were performed in presence of specific activators [Calcium and the reducing agent tris (2-carboxyethyl) phosphine (TCEP) for the calpains activity assay; and 0.01% SDS for the 20S Proteasome activity assay] and inhibitors [the calcium chelator 1,2-bis (o-aminophenoxy) ethane-N,N,N',N'-tetraacetic acid (BAPTA) to inhibit calpain activity and Lactacystin to inhibit proteasome activity, respectively]. The reaction was incubated for 15 minutes at room temperature for calpains activity assay and for 2 hours at 37 °C for the assessment of the proteasome activity. At the end of the reactions we measured the free AMC fluorescence at an excitation wavelength of ~360-380 nm and an emission wavelength of ~440-460 nm. We determined the proteolytic activities by subtracting the activity obtained using the inhibition buffer from the activity detected with the activation buffer.

Optical Mapping Experiments: We performed the optical mapping experiments as we published recently [9]. We used a 16 x 16 photo-diode array with a field-of-view of approximately 2.7 x 2.7 cm to map the entire anterior epicardial surface of the heart. We added the excitation-contraction uncoupler 2,3-butanedione monoxime (BDM, 15mM; Fisher Scientific, Fair Lawn, NJ) to the perfusate in order to suppress the motion artifacts. We then injected voltage-sensitive dye di-4-ANEPPS (Molecular Probes, Eugene, OR) diluted in dimethylsulfoxide (Sigma Aldrich, Inc., St. Louis, MO) into hearts (1.25 mg/ml). We paced the hearts from the anterior left ventricular epicardium midway between the apex and base at a current at least 4 times higher than the pacing threshold. We used an S1-S2 protocol comprised of 20 S1s delivered at a cycle length of 300 ms and S2s with decremental intervals and defined the effective refractory period (ERP) as the last S2 interval to capture.

To determine the vulnerable grid, we applied a train of 20 paced beats at a basic cycle length of 300 ms followed by a truncated exponential monophasic shock (10 ms duration, 80% tilt) at a specified coupling interval (CI) that was randomized within the vulnerable grid. Shock strengths (SS) ranged from approximately 1 V/cm to 18 V/cm. The CI from the last paced beat ranged from 40 to 220 ms with 20 ms steps. We completed the

vulnerable grid for both shock polarities. We used a definition of sustained arrhythmias as arrhythmias lasting more than 6 shock-induced extra-beats. The upper and lower limits of vulnerability (ULV and LLV, respectively) were the highest and lowest SS at which a sustained arrhythmia was induced, respectively. The vulnerable window (VW) was the ULV minus the LLV. The longest and shortest intervals of the vulnerable period (VP) were the longest and shortest CIs which produced a sustained arrhythmia. The VP was the longest minus the shortest extent of VP.

Statistical analysis: We expressed the continuous variables as mean ± SD and determined variance equality or homogeneity by Bartlett's test. We compared the differences among the non-parametric variables with equal variances among the three experimental groups by analysis of variance followed by pair wise comparisons (Bonferroni method). We compared the differences between the baseline and follow up non-parametric parameters by paired t test. We analyzed the differences in the parametric variables among the three groups by the Chi Square test.

Online Supplementary Table 1

Echocardiographic Phenotype at the Beginning (Baseline) and End of the 12-Month (Follow Up) Study

		B-MyHC-Q403		P
	NTG	**Placebo**	**NAC**	
N	10	10	10	
Sex (Male/Female)	6/4	7/3	7/3	0.864
Age (Months)	25.1 ± 6.3	22.2 ± 4.8	23.3±4.1	0.456
BW (Kg)				
Baseline	3.76±0.41	3.70±0.41	3.64±0.22	0.756
Follow up	3.77±0.26	3.87±0.47	3.65±0.34	0.461
Change	-0.04±0.26	0.17±0.14	-0.037±0.18	0.046
P (paired T test)	0.314	0.002	0.292	
Heart Rate (bpm)				
Baseline	130.9±18.5	147.7±12.	140.3±24.4	0.139
Follow up	142.3±32.2	141.0±18.0	146.3±26.6	0.925
Change	15.6±28.8	8.5±22.2	6.4±30.0	0.888
P (paired T test)	0.139	0.137	0.284	
IVST (mm)				
Baseline	2.18±0.20	2.86±0.41	2.87±0.35	0.0002
Follow up	2.10±0.16	3.14±0.38	2.14±0.22	<0.0001
Change	-0.08±0.31	0.28±0.48	-0.73±0.22	0.0001
p (paired T test)	0.219	0.049	<0.0001	
PWT (mm)				
Baseline	2.01±0.22	3.05±0.40	2.53±0.33	<0.0001
Follow up	1.99±0.15	3.03±0.65	2.22±0.30	0.004*
Change	-0.02±0.21	-0.02±0.91	-0.30±0.51	0.607*
P (paired T test)	0.395	0.473	0.071	
LVEDD (mm)				
Baseline	15.33±0.86	14.25±2.24	15.78±1.15	0.191*
Follow up	15.78±0.71	15.51±2.06	15.1±0.88	0.230*
Change	0.45±0.88	1.26±3.12	-0.68±1.03	0.206*
P (paired T test)	0.095	0.145	0.065	
LVESD (mm)				
Baseline	9.74±1.15	8.0±1.79	9.79±0.83	0.014
Follow up	9.40±.91	10.99±1.87	8.54±0.83	0.0007
Change	-0.336±1.43	2.99±2.67	-1.24±1.18	0.0002
p (paired T test)	0.250	0.008	0.010	
LV Mass (g)				
Baseline	3.89±0.35 (3.78; 3.59-4.12)	5.26±1.34 (5.85; 5.37-6.35)	5.72±0.75 (5.98;5.37-6.35)	0.001*
Follow up	3.93±0.51 (3.98; 3.47-4.43)	7.20±2.43 (6.98; 4.45-9.11)	3.86±0.51 (3.88; 3.49-4.24)	0.0002*
Change	0.04±0.57	1.95±2.65	-1.86±0.69	0.0004*

	-0.15; -0.42 – -0.52)	(1.31; -0.26 – 4.47)	(-1.81; -2.53 – -1.28)	
LV Mass/BW (g/Kg)				
Baseline	1.03±0.15 (1.02; 0.89 – 1.52)	1.30±0.56 (1.40; 1.05 – 1.71)	1.56±0.26 (1.63; 1.47 – 1.78)	0.002*
Follow up	1.04±0.12 (1.0; 0.95 – 1.15)	1.80±0.64 (1.79; 1.21 – 2.02)	1.07±0.20 (1.10; 0.91 - 1.24)	0.003*
Change	0.01±0.16 (-0.05; -0.12 – 0.15)	0.50±0.69 (0.44; -0.04 – 1.04)	-0.49±0.21 (-0.46; -0.67 – -0.36)	0.003*
p (paired T test)	0.425	0.023	0.0002	
LVFS (%)				
Baseline	37.22±5.45	35.13±3.04	38.88±1.81	0.056
Follow up	40.34±5.08	29.50±4.28	42.88±4.22	<0.0001
Change	3.12±9.0	-5.62±6.07	4.00±5.26	0.0221
p (paired T test)	0.166	0.017	0.034	
E (cm/s)				
Baseline	49.82±9.25	44.06±10.57	49.28±6.65	0.338
Follow up	41.07±5.80	54.20±8.93	44.51±4.28	0.0009
Change	-8.75±9.48	10.14±12.35	-4.77±5.24	0.0007
p (paired T test)	0.012	0.0145	0.018	
E/A				
Baseline	1.80±0.51	1.50±0.26	1.69±0.52	0.404
Follow up	1.78±0.57	2.24±0.54	1.53±0.34	0.018
Change	-0.016±0.53	0.74±0.61	-0.17±0.45	0.003
p (paired T test)	0.467	0.002	0.167	
IVRT (ms)				
Baseline	46.53±21.1	62.9±12.8	48.3±9.0	0.087
Follow up	50.02±8.27	40.02±7.22	60.04±10.4	0.0004
Change	0.53±27.72	-8.10±10.71	15.46±40.11	0.507*
p (paired T test)	0.201	0.020	0.151	

Abbreviations: BW: Body weight; HR: Heart rate; bpm: Beats per minute; IVST: Interventricular septal thickness; PWT: Posterior wall thickness; LV Mass: Left ventricular mass; LV Mass/BW: Left ventricular mass/body weight; LVEDD: Left ventricular end diastolic diameter; LVESD: Left ventricular end systolic diameter; LVFS: Left ventricular fractional shortening; E/A: Mitral valve inflow early to late velocities; IVRT: Isovolumic relaxation time

* Median values (Median and Q1-Q3 values in parenthesis) were compared by Kruskal-Wallis test.

Figure 1

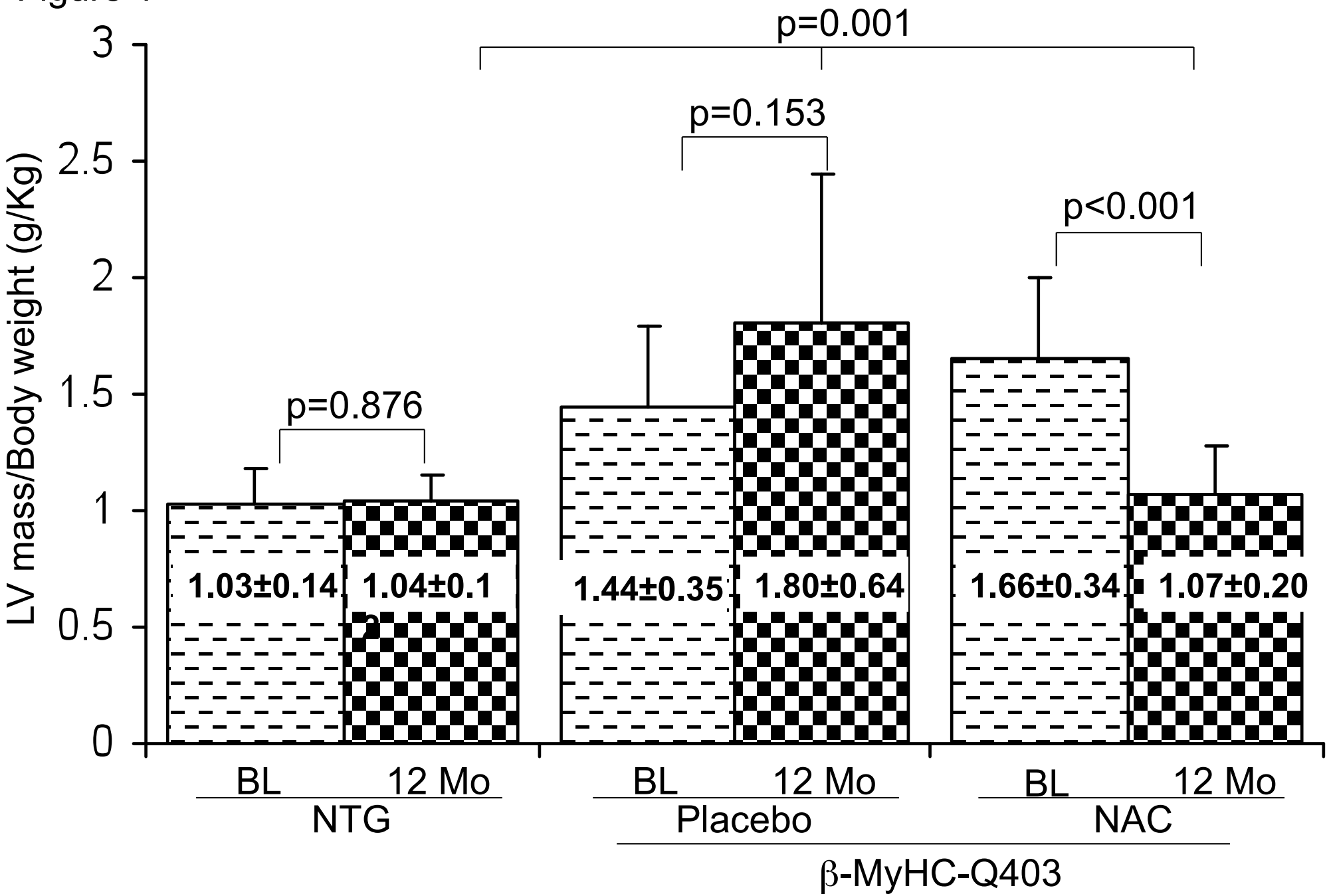
p=0.001
p=0.153
p<0.001
p=0.876
LV mass/Body weight (g/Kg)
3
2.5
2
1.5
1
0.5
0
1.03±0.14
1.04±0.1
2
1.44±0.35
1.80±0.64
1.66±0.34
1.07±0.20
BL
12 Mo
BL
12 Mo
BL
12 Mo
NTG
Placebo
NAC
β-MyHC-Q403

Figure 2

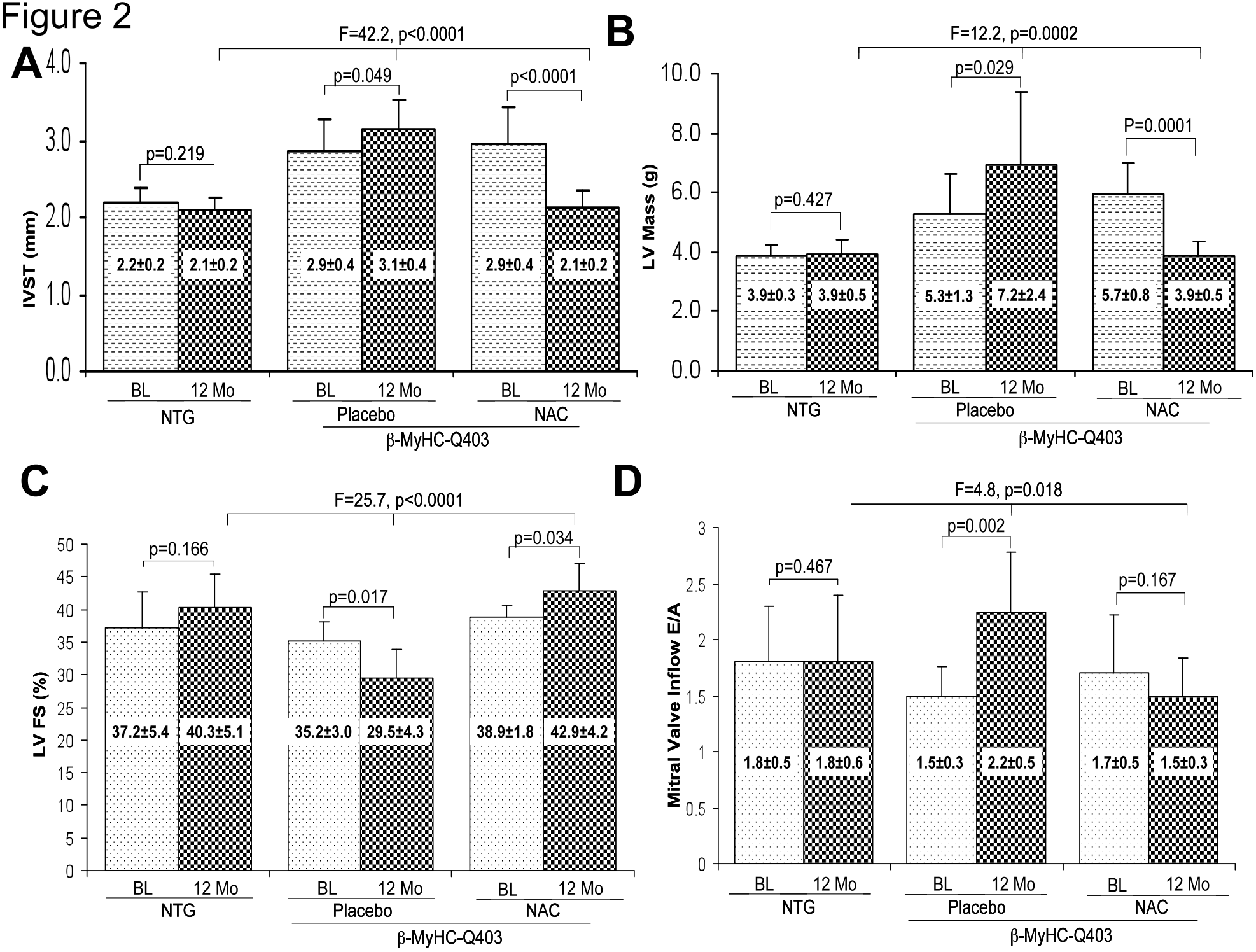
A
F=42.2, p<0.0001
p=0.049
p<0.0001
p=0.219
IVST (mm)
4.0
3.0
2.0
1.0
0.0
2.2±0.2
2.1±0.2
2.9±0.4
3.1±0.4
2.9±0.4
2.1±0.2
BL
12 Mo
BL
12 Mo
BL
12 Mo
NTG
Placebo
NAC
β-MyHC-Q403
B
F=12.2, p=0.0002
p=0.029
P=0.0001
p=0.427
LV Mass (g)
10.0
8.0
6.0
4.0
2.0
0.0
3.9±0.3
3.9±0.5
5.3±1.3
7.2±2.4
5.7±0.8
3.9±0.5
BL
12 Mo
BL
12 Mo
BL
12 Mo
NTG
Placebo
NAC
β-MyHC-Q403
C
F=25.7, p<0.0001
p=0.166
p=0.017
p=0.034
LV FS (%)
50
45
40
35
30
25
20
15
10
5
0
37.2±5.4
40.3±5.1
35.2±3.0
29.5±4.3
38.9±1.8
42.9±4.2
BL
12 Mo
BL
12 Mo
BL
12 Mo
NTG
Placebo
NAC
β-MyHC-Q403
D
F=4.8, p=0.018
p=0.002
p=0.467
p=0.167
Mitral Valve Inflow E/A
3
2.5
2
1.5
1
0.5
0
1.8±0.5
1.8±0.6
1.5±0.3
2.2±0.5
1.7±0.5
1.5±0.3
BL
12 Mo
BL
12 Mo
BL
12 Mo
NTG
Placebo
NAC
β-MyHC-Q403

Figure 3A

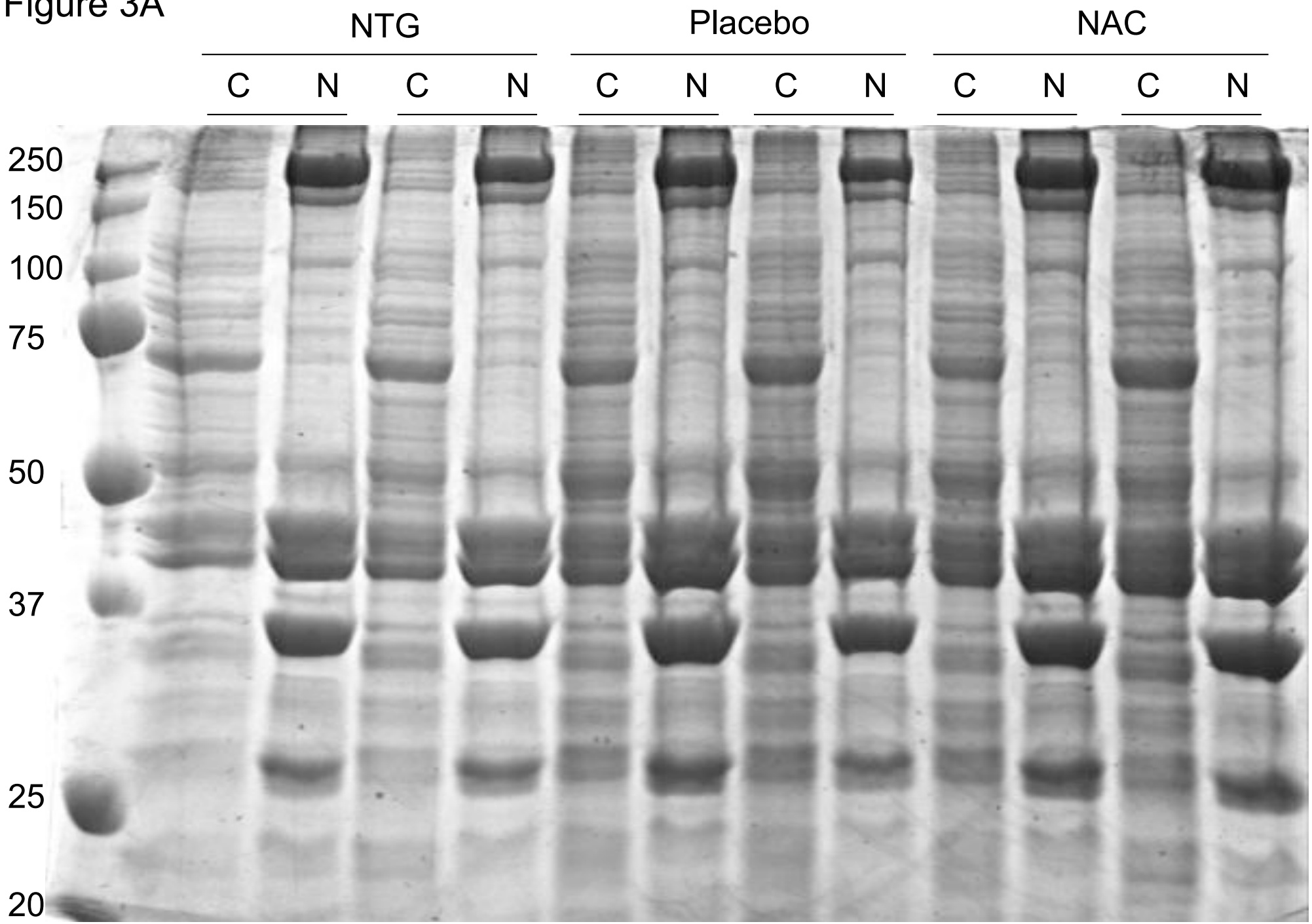

Figure 3B

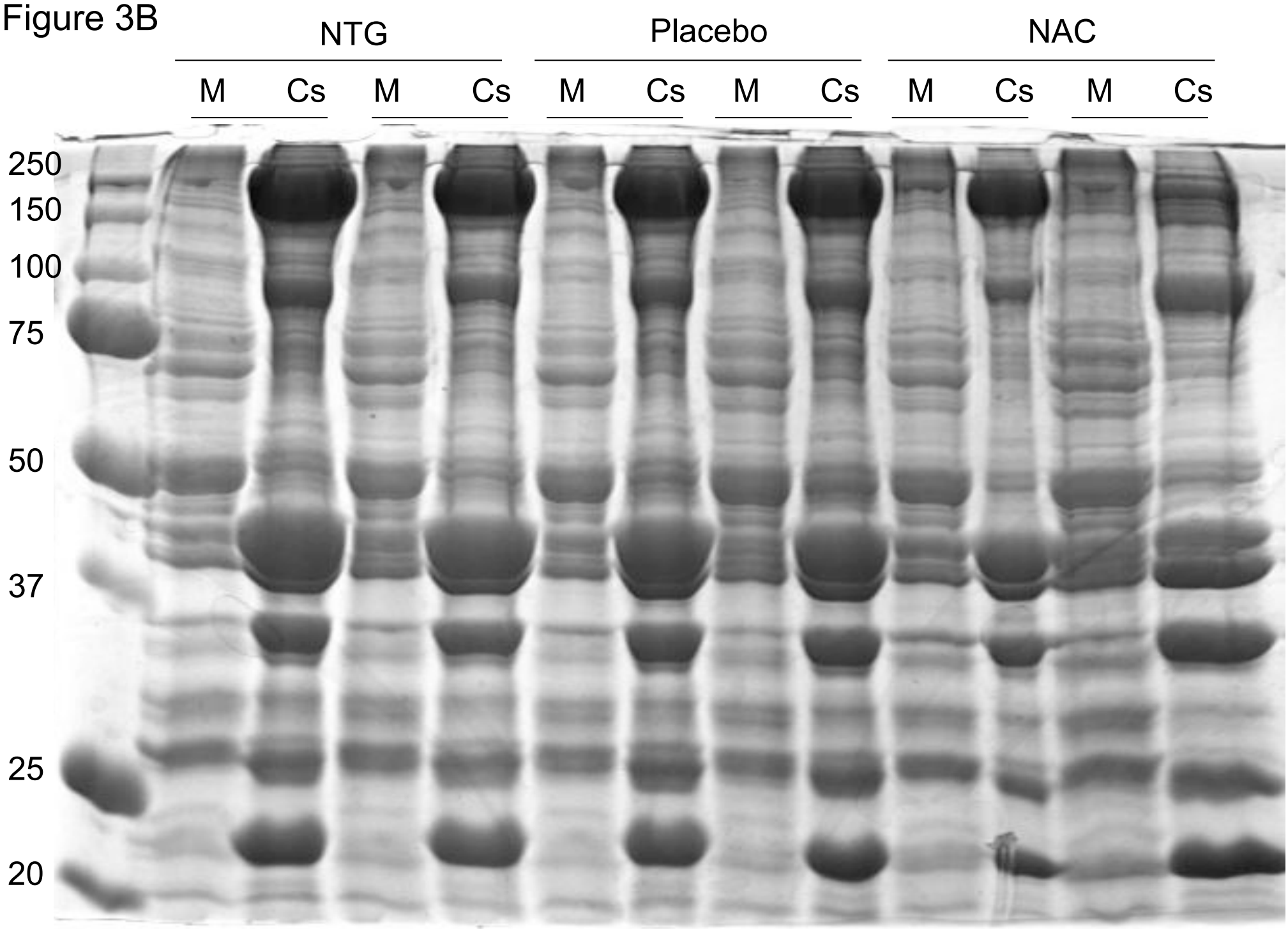
NTG
Placebo
NAC
M
Cs
M
Cs
M
Cs
M
Cs
M
Cs
M
Cs
250
150
100
75
50
37
25
20

Figure 4

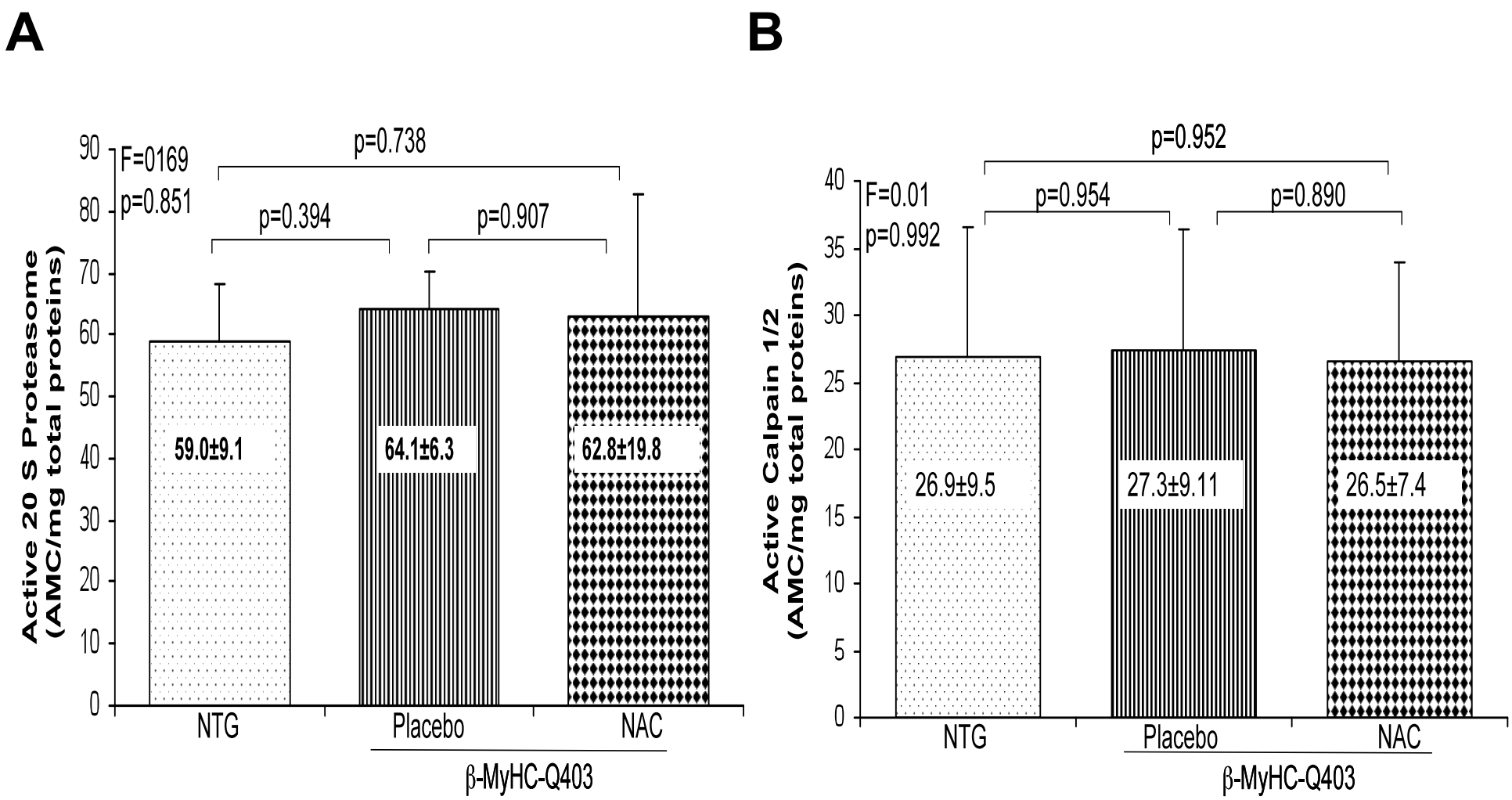
A
F=0169
p=0.851
p=0.738
p=0.394
p=0.907
Active 20 S Proteasome (AMC/mg total proteins)
90
80
70
60
50
40
30
20
10
0
59.0±9.1
64.1±6.3
62.8±19.8
NTG
Placebo
NAC
β-MyHC-Q403
B
F=0.01
p=0.992
p=0.952
p=0.954
p=0.890
Active Calpain 1/2 (AMC/mg total proteins)
40
35
30
25
20
15
10
5
0
26.9±9.5
27.3±9.11
26.5±7.4
NTG
Placebo
NAC
β-MyHC-Q403

Online Supplementary Figure Legends

Figure 1. Interval changes in the primary end point in the β-myosin heavy chain (MyHC)-Q403 transgenic and non-transgenic (NTG) rabbits: Left ventricular mass indexed to body weight (LVM/BW) at the baseline and at follow up in each experimental group is shown. The mean values and standard deviations are shown. Pairwise comparisons are shown along with the comparisons of the LVM/BW indices at the follow up among the three groups by one-way analysis of variance.

Figure 2. Echocardiographic indices of cardiac hypertrophy in the β- MyHC-Q403 transgenic and non-transgenic (NTG) rabbits and their normalization in the N-acetylcysteine (NAC) group.

A. Interventricular septal thickness in mm (IVST); **B.** Left ventricular mass in grams (LV Mass); **C.** Percent left ventricular fractional shortening (LVFS); **D.** Mitral valve inflow E/A ratio. The ANOVA p values reflecting comparison of the three groups at follow up and pairwise p values are shown.

Figure 3. Loading controls for subcellular protein fractionation: Aliquots of 20 μg of each extract were loaded onto 10% SDS-polyacrylamide gels and subjected to electrophoresis for 2 hours. The gels were then stained with Coomassie Blue dye (1X dilution) at room temperature for 2 hours, washed in 1X de-staining solution (50% methanol and 10% acetic acid), soaked in 1% glycerol in ddH_2O for 15 minutes and photographed. Figure 1A represents nuclear (N) and cytosolic (C) protein extracts in 2 rabbits per each of the 3 experimental groups. Figure 1B represent membrane (M) and cytoskeletal (Cs) cardiac protein subfractions in 2 rabbits per group in the three experimental groups.

Figure 4. Proteasomal activities in the hearts of rabbits. Proteasomal activities were determined by spectrophotometric measurement of fluorophore 7-Amino-4- methylcoumarin (AMC) upon release by the cleavage of the substrate Suc-LLVY-AMC in the presence of calpain or 20S Proteasome containing samples. **Panels A** and **B** represent the mean levels

of activities of 20S proteasome and calpain 1/2, respectively, in fresh cardiac protein extracts.

REFERENCES

1. Marian AJ, Wu Y, Lim DS, McCluggage M, Youker K, Yu QT, Brugada R, DeMayo F, Quinones M, Roberts R. A transgenic rabbit model for human hypertrophic cardiomyopathy. *J Clin Invest*. 1999;104:1683-1692.

2. Nagueh SF, Chen S, Patel R, Tsybouleva N, Lutucuta S, Kopelen HA, Zoghbi WA, Quinones MA, Roberts R, Marian AJ. Evolution of expression of cardiac phenotypes over a 4-year period in the [beta]-myosin heavy chain-Q403 transgenic rabbit model of human hypertrophic cardiomyopathy. *Journal of Molecular and Cellular Cardiology*. 2004;36:663-673.

3. Marian AJ, Senthil V, Chen SN, Lombardi R. Antifibrotic Effects of Antioxidant N-Acetylcysteine in a Mouse Model of Human Hypertrophic Cardiomyopathy Mutation. *Journal of the American College of Cardiology*. 2006;47:827-834.

4. Tirouvanziam R, Conrad CK, Bottiglieri T, Herzenberg LA, Moss RB, Herzenberg LA. High-dose oral N-acetylcysteine, a glutathione prodrug, modulates inflammation in cystic fibrosis. *PNAS*. 2006;103:4628-4633.

5. Williams IA, Allen DG. The role of reactive oxygen species in the hearts of dystrophin-deficient mdx mice. *Am J Physiol Heart Circ Physiol*. 2007;293:H1969-H1977.

6. Senthil V, Chen SN, Tsybouleva N, Halder T, Nagueh SF, Willerson JT, Roberts R, Marian AJ. Prevention of Cardiac Hypertrophy by Atorvastatin in a Transgenic Rabbit Model of Human Hypertrophic Cardiomyopathy. *Circ Res*. 2005;97:285-292.

7. Patel R, Nagueh SF, Tsybouleva N, Abdellatif M, Lutucuta S, Kopelen HA, Quinones MA, Zoghbi WA, Entman ML, Roberts R, Marian AJ. Simvastatin induces regression of cardiac hypertrophy and fibrosis and improves cardiac function in a transgenic rabbit model of human hypertrophic cardiomyopathy. *Circulation*. 2001;104:317-324.

8. Nagueh SF, Kopelen HA, Lim DS, Zoghbi WA, Quinones MA, Roberts R, Marian AJ. Tissue Doppler imaging consistently detects myocardial contraction and relaxation abnormalities, irrespective of cardiac hypertrophy, in a transgenic rabbit model of human hypertrophic cardiomyopathy. *Circulation*. 2000;102:1346-1350.

9. Ripplinger CM, Li W, Hadley J, Chen J, Rothenberg F, Lombardi R, Wickline SA, Marian AJ, Efimov IR. Enhanced Transmural Fiber Rotation and Connexin 43 Heterogeneity Are Associated With an Increased Upper Limit of Vulnerability in a Transgenic Rabbit Model of Human Hypertrophic Cardiomyopathy. *Circ Res*. 2007;101:1049-1057.

10. Chen J, Song SK, Liu W, McLean M, Allen JS, Tan J, Wickline SA, Yu X. Remodeling of cardiac fiber structure after infarction in rats quantified with diffusion tensor MRI. *Am J Physiol Heart Circ Physiol*. 2003;285:H946-H954.

11. Hitchcock SE. Actin deoxyroboncuclease I interaction. Depolymerization and nucleotide exchange. *J Biol Chem*. 1980;255:5668-5673.

12. Cox B, Emili A. Tissue subcellular fractionation and protein extraction for use in mass-spectrometry-based proteomics. *Nat Protocols*. 2006;1:1872-1878.